J Fusion Energ
DOI 10.1007/s10894-011-9444-x

ORIGINAL RESEARCH

Practical Optimization of AECS PF-2 Plasma Focus Device for Argon Soft X-ray Operation

M. Akel · S. Lee

Abstract For operation of the plasma focus in argon, a focus pinch compression temperature range of 1.4–5 keV (16.3×10^6–58.14×10^6 K) is found to be suitable for good yield of argon soft X-rays (SXR) Ysxr. This is based on reported temperature measurements of argon plasmas working at regime for X-ray output. Using this temperature window, numerical experiments have been investigated on AECS PF-2 plasma focus device with argon filling gas. The model was applied to characterize the 2.8 kJ plasma focus AECS PF-2. The optimum Ysxr was found to be 0.0035 J. Thus, we expect to increase the argon Ysxr of AECS PF-2, without changing the capacitor bank, merely by changing the electrode configuration and operating pressure. The Lee model code was also used to run numerical experiments on AECS PF-2 with argon gas for optimizing soft X-ray yield with reducing L_0, varying z_0 and 'a'. From these numerical experiments we expect to increase the argon Ysxr of AECS PF-2 with reducing L_0, from the present computed 0.0035 J at $L_0 = 270$ nH to maximum value of near 0.082 J, with the corresponding efficiency is about 0.03%, at an achievable $L_0 = 10$ nH.

Keywords AECS PF-2 · Low energy plasma focus device · Soft X-ray · Argon gas · Lee model RADPF5.15 K

M. Akel (✉)
Department of Physics, Atomic Energy Commission,
P. O. Box 6091, Damascus, Syria
e-mail: pscientific@aec.org.sy

S. Lee
Institute for Plasma Focus Studies, 32 Oakpark Drive,
Chadstone, VIC 3148, Australia

S. Lee
National Institute of Education, Nanyang Technological
University, Singapore 637616, Singapore

S. Lee
INTI International University College, 71800 Nilai, Malaysia

Introduction

Soft X-ray sources of high intensity are required in diverse areas like X-ray spectroscopy [1], lithography for the manufacture of integrated circuits [2], X-ray microscopy [3], X-ray laser pumping [4] and X-ray crystallography [5]. Work is underway to develop such sources by employing geometries like Z-pinch [6], X-pinch [7], vacuum spark [8] and plasma focus (PF) [9–11]. The latter is the simplest in construction and yet provides the highest X-ray emission compared to other devices of equivalent energy [12, 13].

In the last few years various efforts have been made for enhancing the X-ray yield by changing various experimental parameters such as bank energy [14], discharge current, electrode configuration (shape and material) [15, 16], insulator material and dimensions [15], gas composition and filling gas pressure [17]. Thus, soft X-ray yield optimization studies on the plasma focus devices operating over the wide range of bank energies have been one of the actively pursued fields of plasma focus research owing to their vast possible applications.

M. Zakaullah et al. [18, 19] studied the X-radiation emission from a low energy plasma focus with argon as a filling gas. Specifically, attention is paid to determine the system efficiency for argon K-lines and Cu–K_{alpha} line emission at different filling pressures, and identify the radiation emission region. The highest argon line emission

Published online: 24 June 2011

found at 1.5 mbar is about 30 mJ and the corresponding efficiency is 0.0015%.

D. Wong et al. [20] studied the emission characteristics of a high-performance low-energy (3 kJ) repetitive dense plasma focus device, NX2, operated at up to 1-Hz repetition rate to develop it as an intense source of soft X-rays (SXR) for microlithography and micromachining. Various SXR yield optimization studies with argon and neon as filling gases were performed under different operating conditions (charging voltage, filling pressure, anode length, and insulator sleeve length). The SXR yield was computed using signals obtained from a PIN diode SXR spectrometer with appropriate filters. When operated in neon, the average optimum SXR (1 nm) yield in 4 steradians was found to be up to 140 J/shot, which corresponded to a wall plug efficiency of 5.6%. Operation in argon showed that optimized SXR (0.4 nm) yield was up to 1.3 J/shot.

V. A. Gribkov et al. [21] used a dense plasma focus (DPF) as a powerful source of X-rays at the wavelengths useful for microlithography and micromachining depending on its working gas (Ne or Ar correspondingly) and operating parameters of the device.

From the reported experimental results [22], the X-ray emissions from argon plasma are mainly He-like alpha line (He_α ($1s^2$-1s2p, Ar: 3.9488 A° or 3140 eV)) and H-like alpha line (Ly_α (1s-2p, Ar: 3.731 A° or 3323 eV) lines. So the most intense characteristic emissions of argon plasma are Ly_α and He_α lines. The corresponding X-ray emitters in the argon plasmas are mainly H-like and He-like ions.

The corona model [22–25] has been used as an approximation for computing the thermodynamic data of the argon plasma in the plasma focus. Based on the corona model, the ion fraction, effective ionic charge number and effective specific heat ratio for argon plasma have been calculated at different temperatures, for more details see [22]. It is shown that for operation in argon, a focus pinch compression temperature of 1.4–5 keV (16.3×10^6–58.14×10^6 K) is suitable for generating H-like and He-like ions in argon plasma (therefore argon soft X-ray emissions) [22]. This also agrees with the reported temperature measurements with X-ray radiative argon plasma (1.8 keV [26], 1.4–2.4 keV [27], 1–5 keV [28], 1.5–2.5 keV [29]), in which the argon plasma was working around its temperature regime for X-ray output.

In the modified Lee model code version RADPF5.15 K, we take the argon soft X-ray yield (generation H-like and He-like ions) to be equivalent to line radiation yield i.e. $Y_{sxr} = Q_L$ at the following temperature range 1.4–5 keV. The detailed description, theory, latest code and a broad range of results of this 'Universal Plasma Focus Laboratory Facility' are available for download from Ref. [30].

In the present paper, for the first time, we use the latest version Lee Model RADPF5.15 K to carry out the numerical experments on AECS PF-2 [29, 31, 32] device to characterize and compute its argon soft X-ray yield as function of filling gas pressure and then to find the optimum combination of pressure, anode length, and inner radius (p_0, z_0 and 'a') for the maximum soft X-ray yield.

Characterization of AECS PF-2 with Argon Filling Gas

The numerical experiments were investigated on the new relatively low inductance (200 nH) low energy plasma focus device AECS PF-2 for argon soft X-ray optimization. The bank parameters were $L_0 = 200$ nH, $C_0 = 25$ μF and $r_0 = 14$ mΩ. The tube parameters were the outer radius b = 3.2 cm, the inner radius a = 0.95 cm, and the anode length $z_0 = 16$ cm. The operating parameters were $V_0 = 15$ kV, and $p_0 = 0.41$ Torr, filling argon gas.

Several experiments have been investigated on the AECS PF-2 with argon filling gas at wide range of pressures by step 0.1 mbar to get different experimental current traces with good focus effect. By these experiments, the good plasma focus has been obtained at the pressure range from 0.25 to 1.25 Torr, where no focus effect occurs experimentally at higher pressure. To start the numerical experiments we select a discharge current trace of the AECS PF-2 taken with a Rogowski coil at 0.41 Torr. The measured current waveform at the above conditions is shown in Fig. 1.

The computed total current waveform is fitted to the measured waveform as follows:

> We configure the Lee model code (version RADPF5.15 K) to operate as the AECS PF-2 plasma focus starting with the above bank and tube parameters, and then the fitting procedures of the experimental and numerical current traces reported in our recent publication [31] have been used.

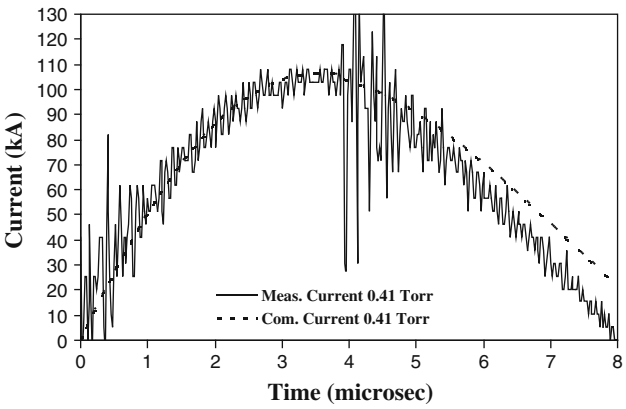

Fig. 1 Comparison of the computed current trace (*dotted line*) with the experimental one (*solid smooth line*) of the AECS PF-2 at 15 kV, 0.41 Torr at argon filling gas

Table 1 Variation AECS PF-2 parameters with pressure at: $L_0 = 270$ nH, $C_0 = 25$ μF, $r_0 = 35$ mΩ, $V_0 = 15$ kV, $c = b/a = 3.368$, RESF = 0.337, $f_m = 0.05$, $f_c = 0.7$, $f_{mr} = 0.15$, $f_{cr} = 0.7$, argon gas

p_0 (Torr)	I_{peak} (kA)	I_{pinch} (kA)	V_a cm/μs	V_s cm/μs	V_p cm/μs	SF	Pinch dur.	Ysxr (J)	Efficiency %
2.2	The code unable to run								
2.00	110	29	2.7	6.7	5.6	82.0	27.3	0	0
1.80	110	37	2.9	9.5	6.5	86.2	19.0	0	0
1.60	110	44	3.2	9.9	7.2	91.3	19.7	0	0
1.40	109	50	3.5	11.1	8.6	97.4	18.0	0	0
1.20	109	57	3.8	13.1	10.9	104.9	15.0	0	0
1.10	109	59	4.0	14.6	12.0	109.4	13.3	0	0
1.00	109	62	4.3	15.9	12.7	114.5	12.2	0	0
0.90	109	65	4.5	17.3	13.7	120.4	11.3	0	0
0.80	108	67	4.8	18.7	14.8	127.4	10.5	0	0
0.60	107	71	5.5	22.9	17.9	146.1	8.8	0	0
0.50	107	72	6.0	25.2	19.4	159.2	8.0	0	0
0.41	106	73	6.5	27.9	21.3	174	7.2	0	0
0.40	106	73	6.6	28.5	21.6	176.9	7.2	0	0
0.30	105	73	7.4	32.9	24.3	202.3	6.2	0	0
0.20	102	71	8.6	39.9	27.7	241.0	5.3	0	0
0.12	97	67	10.3	49.4	31.1	293.7	4.4	0	0
0.1145	96.04	66.59	10.42	49.79	31.29	298.7	4.52	0.0026	0.00009
0.114	95.95	66.54	10.43	49.68	31.33	299.1	4.45	0.0025	0.000089
0.113	95.86	66.47	10.47	49.68	31.39	300.2	4.48	0.0025	0.000089
0.112	95.76	66.40	10.50	49.71	31.46	301.2	4.50	0.0024	0.000086
0.11	95	66	10.6	49.8	31.6	303.1	4.47	0.0023	0.000082
0.10	94	65	10.9	50.0	32.1	313.7	4.44	0.0017	0.000061
0.09	93	64	11.3	50.6	32.7	325.6	4.49	0.0013	0.000046

To obtain a reasonably good fit the following parameters are used [31]:

$$\text{Bank parameters}: L_0 = 270\,\text{nH}, C_0 = 25\,\mu\text{F}, r_0 = 35\,\text{m}\Omega,$$
$$\text{Tube parameters}: b = 3.2\,\text{cm}, a = 0.95\,\text{cm}, z_0 = 16\,\text{cm},$$
$$\text{Operating parameters}: V_0 = 15\,\text{kV}, p_0 = 0.41\,\text{Torr, argon gas},$$

together with the following fitted model parameters:

$f_m = 0.05,\ f_c = 0.7,\ f_{mr} = 0.15$ and $f_{cr} = 0.7$.

With these parameters, the computed total current trace agrees reasonably well with the experimental trace (Fig. 1).

The numerical experiments using RADPF5.15 K at the bank and tube parameters last mentioned above and using the fitted model parameters give then the following results: the end axial speed to be $V_a = 6.5$ cm/μs, the speed factor ($SF = (I_0/ap_0^{1/2})$ is 174 kA/cm per [Torr of argon]$^{1/2}$. The plasma parameters (dimensions, speeds and line radiation) are changing slowly in the first half part of the inward shock phase. The final plasma column is 0.07 cm in radius, and 1.4 cm in length. The inward shock speed is steadily increasing in the inward shock phase to a final on-axis speed of $V_s = 28$ cm/μs and the radial piston speed is also increasing to a maximum value of $V_p = 21$ cm/μs and the pinch duration is about 7 ns. At these experimental conditions was found that no soft X-ray emitted from argon plasma focus (see Table 1). The peak values of total discharge current I_{peak} is about 106 kA, the pinch current I_{pinch} is 73 kA, and the focusing time at about 4 μs.

Optimizing of AECS PF-2 for Argon Soft X-ray Emission

Soft X-ray Yield versus Pressure

These fitted values of the model parameters are then used for the computation of all the discharges at various pressures, fixing all the mentioned above parameters. The pressure was varied from 0.1 to 2.2 Torr.

From Table 1 it is seen that the Ysxr increases with increasing pressure until it reaches the maximum value about 0.003 J at $p_0 = 0.114$ Torr, after which it decreases with higher pressures. As expected as p_0 is increased, the end axial speed, the inward shock speed and the radial

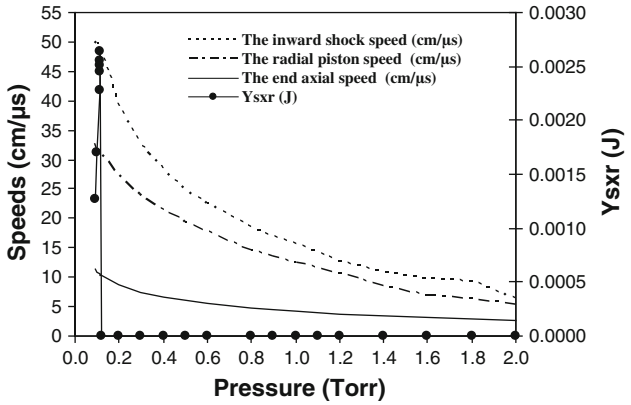

Fig. 2 The X-ray yield, the end axial speed, the inward shock speed and the radial piston speed as functions of the pressure from AECS to PF-2

piston speed all reduced (see Fig. 2). The decrease in speeds lead to lowering of plasma temperatures below that needed for soft X-ray production. From Table 1 we note that a shift of operating pressure to 0.114 Torr would increase the computed Ysxr to 0.003 J at $V_a = 10.42$ cm/μs with the corresponding efficiency is about 0.00009%.

It is also evident from Table 1 that the peak value of total discharge current I_{peak} slightly decreases with decreasing pressure. This is due to increasing dynamic resistance (rate of change of plasma inductance, dL/dt gives rise to a dynamic resistance equal to 0.5 dL/dt) due to the increasing current sheath speed as pressure is decreased. We note that, on the contrary, the current I_{pinch} that flows through the pinched plasma column increases with decreasing pressure until reaches the maximum 73 kA at 0.41 Torr. This is due to the shifting of the pinch time closer and closer towards the time of peak current as the current sheet moves faster and faster [33]. As the pressure is decreased, the increase in I_{pinch} may be expected to favour Y_{sxr}; however, there is a competing effect that decreasing pressure reduces the number density. The interaction of these competing effects will decide on the actual yield versus pressure behavior as shown in the computed results.

Soft X-ray Yield versus Pressure and Electrode Geometry

We next wish to optimize the soft X-ray yield from AECS PF-2 Plasma focus with argon gas, so more numerical experiments were also carried out with the above model parameters; but varying p_0, z_0 and 'a' keeping $c = b/a$ constant at value $c = 3.368$. The pressure p_0 was varied from 0.19 to 2.2 Torr.

The following procedure was used [24]:

- At each p_0, the anode length z_0 was fixed at a certain value,
- Then the anode radius 'a' was smoothly varied, till the maximum X-ray yield (Ysxr) was obtained for this certain value of z_0.
- After that, we chose another value of z_0, varying the value of 'a' looking for the maximum of Ysxr, until we found the optimum combination of z_0 and 'a' for the best X-ray yield at the fixed p_0.
- Then we changed p_0 and repeated the above procedure to find the optimum combination of z_0 and 'a' corresponding to this new value of p_0. We proceed until we had obtained the optimum combination of p_0, z_0 and 'a' for the maximum soft X-ray yield.

The numerical experiments showed that z_0 needed to be increased to optimize the Ysxr (see Table 2). Thus, whilst external inductance L_0 is fixed at a constant value and an axial section inductance L_a is increased due to increasing the anode length, the pinch inductance L_p is reduced due to decreasing the pinch length.

The optimized results for each value of p_0 are shown in Table 2. The table shows that as p_0 is increased, anode length z_0 rises and inner radius 'a' decreases with each increase in p_0, while the soft X-ray yield slightly increases with increasing p_0 until it reaches a maximum value of 0.0035 J at $p_0 = 1.8$ Torr; then the Ysxr decreases with further pressure increase.

Figure 3 shows X-ray yield and the optimum end axial speed as function of p_0, with the plasma focus operated at the optimum combination of z_0 and 'a' corresponding to each p_0.

From the numerical experiments for AECS PF-2 with $L_0 = 270$ nH, $C_0 = 25$ μF, $r_0 = 35$ mΩ, $V_0 = 15$ kV we have thus found the optimum combination of p_0, z_0 and 'a' for argon Ysxr as 1.8 Torr, 24.3 and 0.26 cm, respectively, with the outer radius $b = 0.9$ cm. This combination gives Ysxr = 0.0035 J. We also note that at this optimum configuration $I_{peak} = 102$ kA, $I_{pinch} = 71$ kA, and the end axial speed is of 11 cm/μs.

Practical Optimizing of AECS PF-2 for Argon Soft X-ray Emission

Practically it is technically difficult to change the dimensions of outer radius b; unless the whole electrode system and input flange system of the device is completely redesigned. So, for practical optimization, we wish to continue our numerical experments for argon soft X-ray yield optimization from AECS PF-2, keeping the outer radius fixed at original value of $b = 3.2$ cm and for getting the

Table 2 X-ray yield optimization from AECS PF-2 for each value of p_0 varying z_0 and 'a' at filling argon gas

p_0 (Torr)	z_0 (cm)	a (cm)	I_{peak} (kA)	I_{pinch} (kA)	Ysxr (J)	V_a (cm/μs)	a_{min} (cm)	z_{max} (cm)
0.188	15.5	0.737	95.1	66.1	0.002606	10.36	0.073	1.03
0.263	15.5	0.625	95.3	66.3	0.002650	10.36	0.062	0.88
0.338	15.9	0.555	95.9	66.8	0.002711	10.38	0.055	0.78
0.413	16.0	0.503	96.1	66.9	0.002699	10.38	0.050	0.70
0.488	17.0	0.470	97.6	68.0	0.002931	10.45	0.046	0.66
0.563	17.5	0.441	98.3	68.5	0.003033	10.48	0.044	0.62
0.638	19.5	0.422	100.2	69.8	0.003225	10.61	0.042	0.59
0.713	20.0	0.401	100.6	70.1	0.003264	10.65	0.040	0.56
1.013	20.5	0.338	100.9	70.3	0.003356	10.67	0.033	0.47
1.163	22.5	0.317	101.6	70.8	0.003397	10.82	0.032	0.44
1.400	24.0	0.289	101.7	70.9	0.003464	10.93	0.029	0.41
1.600	24.1	0.271	101.8	70.9	0.003480	10.93	0.027	0.38
1.700	24.3	0.263	101.8	71.0	0.003480	10.94	0.026	0.37
1.800	24.3	0.255	101.8	71.0	0.003481	10.94	0.025	0.36
1.900	25.2	0.248	101.7	70.9	0.003412	11.01	0.025	0.35
2.000	25.5	0.242	101.7	70.9	0.003407	11.03	0.024	0.34
2.200	26.5	0.230	101.7	70.7	0.003384	11.11	0.023	0.32

$L_0 = 270$ nH, $C_0 = 25$ μF, $r_0 = 35$ mΩ, $V_0 = 15$ kV, $c = b/a = 3.368$, $f_m = 0.05$, $f_c = 0.7$, $f_{mr} = 0.15$, $f_{cr} = 0.7$

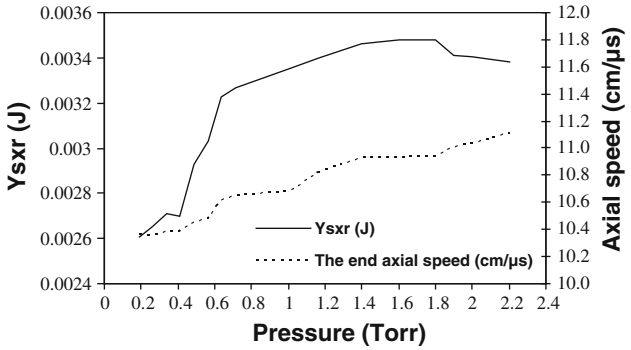

Fig. 3 The X-ray yield and the end axial speed from AECS PF-2 as function of pressure, anode length and inner radius (Ysxr versus p_0, z_0 and 'a')

optimum combinations of (p_0, 'a'), (p_0, z_0) and (p_0, z_0, 'a') for the maximum argon soft X-ray yield.

X-ray Yield Optimization for Each Value of p_0 Varying 'a'

At each p_0, the anode radius 'a' was smoothly varied, till the maximum X-ray yield (Ysxr) was obtained for the original values of $z_0 = 16$ cm and $b = 3.2$ cm. Then we changed p_0 and repeated the above procedure to find the optimum combination of 'a' corresponding to this new value of p_0. We proceed until we had obtained the optimum combination of p_0, 'a' for the maximum soft X-ray yield (see Table 3). The optimum combination of p_0, 'a' for argon Ysxr was found to be 0.41 Torr, $b = 3.2$ cm, $a = 0.532$, $z_0 = 16$ cm. This combination gives Ysxr = 0.00337 J.

X-ray Yield Optimization for Each Value of p_0 Varying z_0

At each p_0, the anode length z_0 was smoothly varied, till the maximum X-ray yield (Ysxr) was obtained for the original value of $a = 0.95$ cm and $b = 3.2$ cm. Then we changed p_0 and repeated the above procedure to find the optimum combination of z_0 corresponding to this new value of p_0. We proceed until we had obtained the optimum combination of p_0, z_0 for the maximum soft X-ray yield (see Table 4). We have also found the optimum combination of p_0, z_0 for argon Ysxr as 0.12 Torr, $b = 3.2$ cm, $a = 0.95$ cm, $z_0 = 18$ cm. This combination gives Ysxr = 0.003 J.

X-ray Yield Optimization for Each Value of p_0 Varying z_0, 'a'

On the other hand, if we keep the outer electrode unchanged and use a screw-on anode, the screw-on part can be designed to be screwed onto an anode stub that keeps the original radius until it just emerges out of the insulator sleeve, at which point it is cut short and has its radius

Table 3 X-ray yield optimization from AECS PF-2 for each value of p_0 varying 'a' at filling argon gas with fixed anode length and outer radius

p_0 (Torr)	z_0 (cm)	a (cm)	I_{peak} (kA)	I_{pinch} (kA)	Ysxr (J)	V_a (cm/μs)	a_{min} (cm)	z_{max} (cm)
0.19	16	0.767	99.2	68.8	0.00298	9.13	0.076	1.07
0.26	16	0.659	100.8	69.9	0.00320	8.30	0.066	0.92
0.34	16	0.585	101.6	70.5	0.00336	7.71	0.058	0.82
0.41	16	0.532	102.0	70.7	0.00337	7.25	0.053	0.74
0.42	16	0.528	102.0	70.7	0.00336	7.22	0.052	0.74
0.49	16	0.489	102.1	70.7	0.00334	6.88	0.049	0.68
0.56	16	0.454	102.3	70.6	0.00335	6.57	0.045	0.64
0.64	16	0.425	102.4	70.4	0.00330	6.30	0.042	0.60
0.71	16	0.401	102.5	70.1	0.00323	6.07	0.040	0.56
1.01	16	0.327	102.9	68.2	0.00297	5.36	0.032	0.46
1.16	16	0.301	103.0	67.2	0.00272	5.09	0.030	0.42

Table 4 X-ray yield optimization from AECS PF-2 for each value of p_0 varying z_0 at filling argon gas with fixed inner and outer radiuses

p_0 (Torr)	z_0 (cm)	a (cm)	I_{peak} (kA)	I_{pinch} (kA)	Ysxr (J)	V_a (cm/μs)	a_{min} (cm)	z_{max} (cm)
0.100	13.0	0.95	89.6	62.2	0.0020	10.2	0.094	1.33
0.120	18.0	0.95	98.7	68.3	0.0030	10.6	0.094	1.34
0.130	23.0	0.95	101.7	70.3	0.0000	10.9	0.094	1.33
0.150	22.0	0.95	102.4	70.7	0.0000	10.2	0.089	1.33
0.188	20.0	0.95	103.4	71.4	0.0000	9.2	0.082	1.34
0.263	17.0	0.95	104.8	72.3	0.0000	7.9	0.073	1.35
0.338	15.0	0.95	105.6	72.9	0.0000	7.0	0.069	1.36
0.410	14.0	0.95	106.3	73.3	0.0000	6.4	0.066	1.36
0.418	13.5	0.95	106.3	73.4	0.0000	6.3	0.066	1.35
0.488	13.0	0.95	106.9	73.7	0.0000	5.9	0.063	1.36
0.563	12.5	0.95	107.3	73.9	0.0000	5.5	0.060	1.37
0.638	11.1	0.95	107.6	74.2	0.0000	5.2	0.055	1.38
0.713	11.0	0.95	107.9	74.4	0.0000	4.9	0.048	1.40
1.013	9.8	0.95	108.8	74.7	0.0000	4.2	0.015	1.76
1.163	9.0	0.95	109.1	75.0	0.0000	3.9	0.017	1.86

converted to that of the screw-on part. Then the screw-on part of the anode can have the optimized radius '*a*' and anode length z_0.

Keeping b = constant at the original value of 3.2 cm; changing 'a' to 0.255 cm with $z_0 = 24.3$ cm; and varying pressure to find this 'practical optimum'. This gives us a practical optimum configuration of b = 3.2 cm (unchanged from the original cathode radius of the standard AECS PF-2), a = 0.255 cm, $z_0 = 24.3$ cm, giving a practical optimum yield of 0.001 J at a P_0 of 1 Torr. The slightly lower yield compared with that in Table 1 is due to the increased ratio "c" from 3.4 to 12.5.

The optimum combination of p_0, z_0, 'a' for argon Ysxr as 1.3 Torr, b = 3.2 cm, a = 0.3 cm, $z_0 = 11$ cm. This combination gives Ysxr = 0.0037 J (see Table 5).

Nevertheless the numerical experiments have shown that with the present capacitor bank, AECS PF-2 plasma focus has a maximum Ysxr at about 0.0037 J.

Soft X-ray Yield versus Inductance and Electrode Geometry

To optimize the soft X-ray yield from AECS PF-2 with argon gas, varying L_0, z_0 and 'a' keeping 'c' and RESF constant. The external inductance L_0 was varied from 200 to 1 nH.

The following procedures were used [25, 32]:

At each L_0, the pressure was fixed at constant value (in our case $p_0 = 0.41$ Torr) and also the anode length was fixed at a certain value:

Table 5 X-ray yield optimization from AECS PF-2 for each value of p_0 varying z_0 and 'a' at filling argon gas with fixed outer radius

p_0 (Torr)	z_0 (cm)	a (cm)	I_{peak} (kA)	I_{pinch} (kA)	Ysxr (J)	V_a (cm/μs)	a_{min} (cm)	z_{max} (cm)
0.26	18.0	0.663	101.6	70.4	0.00327	8.5	0.066	0.93
0.41	15.5	0.532	101.9	70.7	0.00338	7.2	0.053	0.75
0.49	17.0	0.487	102.1	70.4	0.00336	6.9	0.048	0.68
0.56	16.0	0.454	102.3	70.6	0.00335	6.6	0.045	0.64
0.71	12.5	0.408	102.6	71.3	0.00354	5.9	0.040	0.57
1.01	12.0	0.344	103.2	71.6	0.00356	5.2	0.034	0.48
1.05	12.0	0.337	103.2	71.6	0.00357	5.1	0.034	0.47
1.13	11.0	0.327	103.3	71.9	0.00360	5.0	0.033	0.46
1.20	10.5	0.317	103.4	71.9	0.00366	4.8	0.031	0.45
1.30	11.0	0.305	103.6	71.9	0.00367	4.7	0.030	0.43

Table 6 For each L_0 the optimization combination of z_0 and 'a' were found and are listed here

L_0 (nH)	z_0 (cm)	a (cm)	b (cm)	I_{peak} (kA)	I_{pinch} (kA)	a_{min} (cm)	Z_{max} (cm)	V_a (cm/μs)	Ysxr (J)	Efficiency %
270	26.00	0.53	1.79	102	70.5	0.05	0.74	11.12	0.0034	0.00012
200	23.00	0.60	2.02	116	79.8	0.06	0.84	11.23	0.0055	0.00019
100	9.20	0.75	2.51	145	99.6	0.08	1.05	10.59	0.013	0.0046
50	7.60	0.97	3.27	197	130.5	0.10	1.37	11.26	0.035	0.013
20	7.40	1.21	4.07	273	165.4	0.14	1.73	13.21	0.075	0.027
15	6.80	1.25	4.20	294	172.0	0.15	1.79	13.85	0.08	0.028
10	6.40	1.28	4.31	320	177.9	0.17	1.85	14.90	0.082	0.029
5	6.20	1.29	4.34	355	181.0	0.18	1.88	16.60	0.078	0.028
1	6.17	1.25	4.21	397	177.3	0.18	1.84	18.54	0.066	0.024

Bank parameters: $L_0 = 270$ nH, $C_0 = 25$ μF, $r_0 = 35$ mΩ; tube parameter: $c = b/a = 3.368$; model parameters: $f_m = 0.05$, $f_c = 0.7$, $f_{mr} = 0.15$, $f_{cr} = 0.7$; operating at 0.41 Torr argon gas, $V_0 = 15$ kV

- Then the inner radius 'a' was varied, whilst keeping $c = 3.368$, until the maximum X-ray yield was obtained for this certain value of z_0.
- After that we chose another value of z_0, varying 'a' until maximum X-ray yield and so on, until we have obtained the combination of z_0 and 'a' for the best maximum X-ray yield at a fixed L_0 (Ysxr vs. z_0 and 'a' at fixed L_0 and p_0).
- We repeated the above procedure for progressively smaller L_0 until $L_0 = 1$nH.

The influence of L_0 reduction on the total current traces using RADPF5.15 K was investigated. For example it was found that reducing L_0 increases the total current from $I_{peak} = 102$ kA at $L_0 = 270$ nH to $I_{peak} = 294$ kA at $L_0 = 15$ nH (see Table 6). As L_0 was reduced, I_{peak} increased; 'a' is necessarily increased leading to longer pinch length (Z_{max}), hence a bigger pinch inductance L_p. At the same time because of the reducing current drive time, z_0 needed to be reduced. The geometry moved from a long thin Mather-type to a shorter fatter one (see Table 6). Thus, whilst L_0 and axial section inductance L_a reduced, the pinch inductance L_p increased due to increased pinch length.

At each L_0, after z_0 was varied, the inner radius 'a' was adjusted to obtain the optimum X-ray yield, which corresponds closely to the largest I_{pinch}.

The soft X-ray optimization for each value of L_0, varying z_0 and 'a' is shown in Table 6. The table shows that as L_0 is reduced, I_{peak} increases with each reduction in L_0 with no sign of any limitation as function of L_0. However, I_{pinch} reaches a maximum of 181 kA at $L_0 = 5$ nH, then it decreases with each reduction in L_0. Thus, I_{peak} doesn't show any limitation as L_0 is progressively reduced. However, I_{pinch} has a maximum value. This pinch current limitation effect is not a simple, but it is a combination of the two complex effects: the interplay of the various inductances involved in the plasma focus processes abetted by the increasing coupling of C_0 to the inductive energetic processes, L_0 is reduced.

From Table 6 it can be seen, that as L_0 decreased, the soft X-ray yield increases until it reaches a maximum value of 0.0823 J at $L_0 = 10$ nH, with the corresponding efficiency is about 0.03%.; beyond which the soft X-ray yield and the corresponding efficiency do not increase with reducing L_0. Thus, with decreasing L_0 the pinch current I_{pinch} and the soft X-ray yield show limitation. The

obtained results confirm the pinch current limitation effect in argon plasma focus, and consequently the soft X-ray yield.

Looking at Table 6, it is noticed that as L_0 was progressively reduced, to optimize 'a' had to be progressively increased and z_0 progressively decreased. Also the plasma pinch dimensions (pinch radius a_{min} and pinch length Z_{max}) increased as L_0 was reduced.

Based on the obtained results of these sets of numerical experiments on AECS PF-2 with argon gas, we can say that to improve the soft X-ray yield, L_0 should be reduced to a value around 10–20 nH (which is an achievable range incorporating low inductance technology, below which the pinch current I_{pinch} and the soft X-ray yield Ysxr would not be improved much, if at all. These experiments confirm the pinch current limitation effect, and consequently the soft X-ray yield for the argon plasma focus. Finally, we would like to emphasize that we, practically, have no intention (or ambition) to go below 10–15 nH (which is an achievable range), but in our numerical experiments using RADPF5.15 K we go down to a low values of L_0 (8–1 nH) just to find the pinch current limitation effect.

Conclusions

The Lee model code was applied to characterize the AECS PF-2 Plasma Focus, finding a maximium argon soft X-ray yield (Ysxr) of 0.0026 J, merely by changing the operating pressure. The argon soft X-ray optimum combination of AECS PF-2, found to be (pressure = 1.8 Torr, anode length = 24.3 cm and anode radius = 0.255 cm). The optimum Ysxr was 0.0035 J.

Numerical experiments have been investigated on AECS PF-2 with argon gas for optimizing soft X-ray yield with reducing L_0, varying z_0 and 'a'. From these numerical experiments we expect to increase the argon Ysxr of AECS PF-2 with reducing L_0, up to 0.082 J at the operating pressure 0.4125 Torr with efficiency $\sim$0.03%.

Acknowledgments The authors would like to thank Director General of AECS, for encouragement and permanent support. The authors would also like to express thanks to Prof. Dr. Sharif Al-Hawat, who provide us with experimental current traces of argon AECS PF-2. The first author would also like to express thanks to Mrs. Sheren Isamael, who collaborated going through all the numerical experiments using Lee Model.

References

1. J.S. Pearlman, J.C. Roirdan, J. Vac. Sci. Technol. **19**, 1190 (1981)
2. R. Feder, J.S. Pearlman, J.C. Riordan, L.J. Costa, J. Microsc. **135**, 347 (1984)
3. B. Niemann et al., Optik **84**, 35 (1989)
4. J.L. Porter et al., Phys. Rev. Lett. **68**, 796 (1992)
5. J.J. Rocca et al., Phys. Rev. Lett. **73**, 2192 (1994)
6. V.L. Kantsyrev. et. al. in *Proceedings 3rd International Conference on Dense Z-pinches (London, UK)*, vol. 299, ed. by M. Haines, A. Knight (AIP, New York, 1993), p. 226
7. D.A. Hammer et al., Appl. Phys. Lett. **57**, 2083 (1990)
8. A. Ikhlef, et. al. in *Proceedings 3rd International Conference on Dense Z-pinches (London, UK)*, vol. 299, ed by M. Haines, A. Knight (AIP, New York, 1993), p. 218
9. C.S. Wong, S. Lee, Rev. Sci. Instrum. **55**, 1125 (1984)
10. J.W. Mather, Phys. Fluids **8**, 366 (1965)
11. M. Zakaullah et al., Phys. Plasmas **6**, 3188 (1999)
12. M. Zakaullah et al., Appl. Phys. Lett. **78**, 877 (2001)
13. S. Lee et al., IEEE Trans. Plasma Sci. **26**, 1119 (1998)
14. S. Lee et al., Plasma Phys. Control. Fusion **51**, 105013 (2009)
15. M. Zakullah et al., Plasma Sour. Sci. Technol **11**, 377 (2002)
16. H. Bhuyan et al., J. Appl. Phys **95**, 2975 (2004)
17. F.N. Beg et al., J. Appl. Phys **88**, 3225 (2000)
18. M. Zakaullah, et. al. IEEE Trans. Plasma Sci. **30**(6):2089 (2002)
19. M. Zakaullah et al., Plasma Sour. Sci. Technol **9**, 592–596 (2000)
20. D. Wong et al., IEEE Trans. Plasma Sci. **32**, 6 (2004)
21. V.A. Gribkov et al., IEEE Trans. Plasma Sci. **30**, 3 (2002)
22. S. Bing, *Plasma dynamics and x-ray emission of the plasma focus.* PhD Thesis. NIE ICTP Open Access Archive: http://eprints.ictp.it/99/ (2000)
23. M.H. Liu, *Soft X-Ray from Compact Plasma Focus*. PhD Thesis, School of Science, Nanyang Technological University (Dec 1996)
24. M. Akel, Sh. Al-Hawat, S. Lee, J. Fusion Energ. **28**(4), 355–363 (2009)
25. M. Akel, Sh. Al-Hawat, S. Lee, J. Fusion Energ. **29**, 1 (2010)
26. T. Yanagidaira, T. Yamamoto, B. Shan, K. Hirano, Spectroscopic investigation of z-pinch with a spatial and temporal resolution. J. Phys. Soc. Jpn **68**, 852–856 (1999)
27. S.R. Mohanty, M.P. Srivastava, R.S. Rawat, Phys. Lett. A **234**, 472–476 (1997)
28. S.P. Moo, C.S. Wong, A.C. Chew, S. Lee, 12 years of research and training with the UNU/ICTP PFF at the university of Malaya, in *Twelve Years of UNU/ICTP PFF: A Review* (1998)
29. Sh. Al-Hawat, M. Akel, C.S. Wong, J. Fusion Energ. doi: 10.1007/s10894-011- 9417-0 (2011)
30. S. Lee, *Radiative Dense Plasma Focus Computation Package: RADPF*. http://www.intimal.edu.my/school/fas/UFLF/. http://www.plasmafocus.net/IPFS/modelpackage/File1RADPF.htm. (2011)
31. Sh. Al-Hawat, M. Akel, S. Lee, S.H. Saw, J. Fusion Energ. doi: 10.1007/s10894-011-9414-3 (2011)
32. Sh. Al-Hawat, M. Akel, S. Lee, J. Fusion Energ. doi:10.1007/s10894-011-9416-1 (2011)
33. S.H. Saw et al., IEEE Trans. Plasma Sci. **37**(7), 1276–1282 (2009)